X-650-73-194
PREPRINT

66291

DYNAMICS AND MORPHOLOGY OF BEAUFORT SEA ICE DETERMINED FROM SATELLITES, AIRCRAFT, AND DRIFTING STATIONS

W. J. CAMPBELL
P. GLOERSEN

JUNE 1973

GSFC — GODDARD SPACE FLIGHT CENTER —
GREENBELT, MARYLAND

COLOR ILLUSTRATIONS REPRODUCED IN BLACK AND WHITE

A.5.6

X-650-73-194

DYNAMICS AND MORPHOLOGY OF BEAUFORT SEA ICE DETERMINED FROM SATELLITES, AIRCRAFT, AND DRIFTING STATIONS

by

W. J. Campbell,* P. Gloersen, W. Nordberg, and T. T. Wilheit

NASA Goddard Space Flight Center

Greenbelt, Maryland 20771 U.S.A.

and

*U.S. Geological Survey, University of Puget Sound

Takoma, Washington, U.S.A.

June 1973

GODDARD SPACE FLIGHT CENTER

Greenbelt, Maryland

DYNAMICS AND MORPHOLOGY OF BEAUFORT SEA ICE DETERMINED FROM SATELLITES, AIRCRAFT, AND DRIFTING STATIONS

W. J. Campbell, P. Gloersen, W. Nordberg, and T. T. Wilheit

ABSTRACT

A series of measurements from drifting stations, aircraft, the ERTS-1, Nimbus 4, and Nimbus 5 satellites have jointly provided a new description of the dynamics and morphology of the ice cover of the Beaufort Sea. The combined analysis of these data show that the eastern Beaufort Sea ice cover is made up of large multiyear floes while the western part is made up of small, predominantly first-year floes. The analysis suggests that this distribution might be quasi-steady-state and that the dynamics and thermodynamics of the region are more complex than hitherto known. The measurements consist of: (1) high resolution ERTS-1 imagery which is used to describe floe size and shape distribution, short term floe dynamics, and lead and polynya dynamics; (2) tracking by Nimbus 4 of IRLS drifting buoys to provide ice drift information which enhances the interpretation of the ERTS-1 imagery; (3) Nimbus 5 microwave (1.55 cm wavelength) imagery which provides synoptic, sequential maps on the distribution of multiyear and first-year ice types; (4) airborne microwave surveys and surface based observations made during 1971 and 1972 in conjunction with the AIDJEX (Arctic Ice Dynamics Joint Experiment) program.

CONTENTS

DYNAMICS AND MORPHOLOGY OF BEAUFORT SEA ICE DETERMINED FROM SATELLITES, AIRCRAFT, AND DRIFTING STATIONS

INTRODUCTION

Strong interest in sea ice was generated by the results of recent climate models, such as Mintz (1965), Budyko (1968, 1969), and Fletcher (1965, 1968), indicating that because of the effect of sea ice on the heat budget of the Arctic the distribution and amount of sea ice is an important and possibly a major influence in the climate of the Northern Hemisphere. Fletcher (1968) points out that sea ice distribution in both the Arctic and Antarctic should be monitored as an indicator of changes in oceanic heat exchange.

During the 1960's, it became obvious that observations from the traditional single drifting stations were intrinsically inadequate in providing sufficient data on the complex air-ice-ocean interaction of the Arctic Ocean with which to test the developing large scale numerical models of the ice canopy. Several investigators, such as Laikhtman (1958), Ruzin (1959), and Campbell (1965), developed mathematical models which indicated that a force neglected in earlier models, the internal ice force generated by momentum exchange between the ice floes, was a dominant one and must be included in any realistic model for sea ice dynamics. Recently, two new observing techniques, both derived from the space program, made possible the inference of the rheological properties of sea ice over vast areas, namely simultaneous measurements of ice, water, and air motion from an array of drifting stations relayed by satellites and the satellite acquisition of sequential, synoptic images of radiation emitted and reflected

by sea ice which relate to the dynamics of floes, leads, polynyas, and ridges.

Sunlight and infrared observations of the Arctic ice canopy obtained by early meteorological satellites (Nelson et al. 1970, Campbell 1971, McClain and Baliles 1971, Barnes et al. 1972) revealed that it undergoes large scale space variations at small time scales and is the most variable solid feature of the earth's surface. However, these early observations were of low resolution; thus, individual ice floe trajectories and the dynamics of leads and polynyas could not be studied with them. Because the Arctic is dark for many months and often cloud covered when sun lit, it was not possible to obtain an adequate sequential view using visible and infrared images. Furthermore, these early data were not coupled with detailed surface (ground truth) observations.

In 1970 an international and interdisciplinary Arctic Ice Dynamics Joint Experiment (AIDJEX) was formed with the objective of reaching, through coordinated field experiments and theoretical analysis, a fundamental understanding of the dynamic and thermodynamic interaction between Arctic sea ice and its environment. AIDJEX launched three spring pilot experiments in the Beaufort Sea in 1970, 1971, and 1972, in which surface based measurements were combined with photographic, infrared and microwave observations made during overflights with the NASA Convair 990 aircraft. Some of these observations were described by Wilheit et al., 1972; Campbell, 1973; and Gloersen et al., 1973. Subsequent to these experiments which combined very effectively airborne remote sensing with extensive surface measurements, very detailed images of Beaufort Sea ice from the ERTS-1, synoptic microwave pictures of the entire Arctic from Nimbus 5, and tracking of automatic platforms on the ice from

Nimbus 4 became available. In this paper, we wish to show how the combination of data from surface experiments, aircraft, and these three satellites have given us a new understanding of the sea ice of the Beaufort Sea.

AIRCRAFT MICROWAVE AND SURFACE OBSERVATIONS OF SEA ICE

Remote sensing from the NASA CV-990 aircraft flown in conjunction with the AIDJEX 1970, 1971, and 1972 pilot experiments involved 14 overflights of AIDJEX areas, numerous flights over the transition zone extending from the north coast of Alaska out to the active sea ice, and one extending from 75°N to the conjectured steady-state center of the Beaufort Sea Gyre (Figure 1).

The 1970 experiment showed that by mapping microwave emission at 1.55 cm wavelength, it was possible to distinguish ice from liquid water under all meteorological conditions during all seasons (Wilheit et al., 1972). This finding was of great importance from both the dynamic and thermodynamic viewpoints. Strong microwave emissivity differences amounting to about 20°K in brightness temperature between two types of ice were also apparent in these observations. The 1971 AIDJEX-NASA experiment was designed to shed some light on the phenomenon of these varying microwave emissivities. High altitude flights were conducted to obtain images of the largest possible area of sea ice by flying overlapping parallel flight lines, and two microwave images of a 93 km by 93 km area of ice were obtained under clear and cloudy conditions. Gloersen et al., (1972) showed that the varying ice emissivities were due to varying ice types, with the cold brightness temperatures corresponding to multiyear ice (thickness of two or more meters, low salinity, many empty brine inclusions near the surface, refrozen crystals) and the warmer brightness temperatures corresponding to

first-year ice (less than two meters thick, high salinity, most brine inclusions full, crystals of the original freezing). This demonstrated an all-weather capability of distinguishing multiyear and first-year ice over a large area of the Arctic.

One of the microwave mosaic images from this study is shown in Figure 2. The AIDJEX camp, where most of the surface-based measurements were made, is shown by a white circle. It was located on the north edge of a very large multiyear ice floe in the eastern Beaufort Sea (Figure 1). This large floe as well as numerous smaller ones appear in the image as having a low brightness temperature (blue, dark green), whereas the first-year ice has a high brightness temperature (yellow, orange). The white triangle to the northeast of the camp indicates the position of the CRREL tellurometer strain array (Hibler et al., 1972) which was situated entirely on first-year ice with a thickness of from 1.3 to 2.0 meters, having only small ridges and leads at the time of observation. The extensive ground truth and microwave measurements during the AIDJEX-NASA 1971 experiment served to correlate definitely the signatures to varying ice types.

The 1972 AIDJEX Pilot Experiment was considerably more extensive than the 1971 experiment. The area of study was several hundred kilometers further west of the 1971 site (Figure 1). Three manned stations were occupied for two months and seven unmanned AIDJEX-IRLS drifting buoys, left in place at the termination of the main experiment, were placed at ranges of about 400 km around the manned array (positions and drift trajectories are shown in Figure 6). High level microwave mosaic images of the area encompassing the three manned stations (Gloersen et al., 1972) were obtained; part of one is shown in Figure 2, in

comparison with an image of an equally-sized area obtained a year earlier in the eastern Beaufort Sea.

The most startling difference between these images of a large area of sea ice in the western Beaufort Sea and that of an equal area in the eastern Beaufort Sea obtained a year earlier is that there are no large multiyear ice floes in the western sector as there were earlier in the eastern sector at the same latitude. Surface measurements obtained by participants in the 1972 experiment (Hibler et al., 1973) showed that the main camp was located on a floe made up of cemented pieces of first-year and multiyear ice, but the amount of multiyear ice was apparently less than that of first-year ice; therefore the integrated signature over the area of the radiometer footprint (500 m $\times$ 500 m) appears radiometrically to be first-year ice. An area of 1.1×10^4 m^2 of sea ice adjacent to the main camp containing both ice types was studied in great detail (Meeks et al., 1972) by measuring the surface microwave emissivities at 13.4 GHz in a grid of forty-four points along with ice crystalographic sampling, and the average brightness temperature of those points was found to be that of first-year ice, in agreement with observation of that area obtained from the aircraft. The microwave images show that there was significantly more first-year than multiyear ice and that there definitely were no large multiyear floes. According to the brightness temperatures observed, there could not have been more than 10% multiyear ice in the area.

This was surprising because it was generally believed that the ratio of old and new ice was fairly homogeneous throughout the Arctic Basin, with the exception of coastal areas. To find such a large area of predominantly first-year ice so deep within the ice pack contradicted long held thermodynamic and dynamic

beliefs. Therefore, after these findings had been obtained from four successive flights over the AIDJEX array, we decided to fly a mission covering an area extending from the array to as deep within the Beaufort Sea Gyre as logistical constraints permitted. The microwave image obtained is shown in Figure 3, and the position of the area is shown in Figure 1. The image shows that just north of the AIDJEX array there were small multiyear floes (low brightness temperatures) with larger ones starting at 76°45'N latitude and continuing until 79°N. North of 79°N the pack was essentially solid multiyear ice. The linearments of high brightness temperatures in this area are due to new ice covering recently refrozen leads and polynyas. No large multiyear floes similar to those observed a year earlier in the eastern Beaufort Sea were observed along this entire pass.

Figure 4 shows that microwave images can be used to study ice dynamics. The dark green linear features are new leads, some being narrower than 500 meters and therefore not fully covering the radiometer footprint, having a preferred SE-NW orientation in the left image. The right image shows the same area three days later, during which period a strong cyclone passed south of the AIDJEX array, and the lead orientation has switched almost orthogonally to a SW-NE direction.

ERTS-1 OBSERVATIONS OF BEAUFORT SEA ICE MORPHOLOGY

Although important studies of sea ice were made using data from meteorological satellites, such as Nelson et al. (1970), McClain and Baliles (1971), and Barnes et al. (1972), it was not until the launching of ERTS-1 that imagery of sufficiently high resolution was available to allow the delineation of individual floes, leads, and polynyas. A limited amount of images from ERTS-1 of the

Beaufort Sea was available to us for the period from late July until mid-October 1972. On 22 August 1972, ERTS-1 obtained images from both the eastern and western Beaufort Sea, roughly in the same area as the 1971 and 1972 overflights had been conducted. Figure 5c shows the ERTS-1 image strip (160 km × 480 km) of the eastern Beaufort Sea. Very large, round shaped ice floes cover most of the area, some as large as 55 km across and ten more than 35 km across. These same floes can be identified in images (not shown) obtained on 2 August; in the three-week summer period between these observations they underwent very little weathering while moving towards the southwest, with only a few showing any discernable change of shape. The longest time sequence of ERTS-1 images covering one set of flows extended from 17 August to 24 September 1972 and consists of five passes over an area just east of the center of the 1971 AIDJEX grid. Two large floes (13 km × 28 km and 16 km × 27 km) could be tracked during the five and one-half week period and one showed no signs of weathering. The drift trajectories of these two floes as derived from ERTS-1 images are shown in Figures 1 and 6. A later image obtained on 12 October in the same area again shows numerous large round floes.

The shape and size of the large floes observed in the eastern Beaufort Sea resemble those of the multiyear floes shown in microwave images obtained in the same area in 1971 (Figure 2). Although we cannot positively say that these large floes were indeed multiyear floes, the fact that they endured a summer melt season and much dynamic activity while undergoing only minor weathering strongly suggests that they were.

Also on 22 August 1972, 100 minutes after the images comprising Figure 5c were obtained, ERTS-1 overflew the western Beaufort Sea, and obtained the

image strip, shown in Figure 5a, in approximately the same geographic area where the 1972 experiment took place. The most striking difference between this strip and the one shown in Figure 5c is the complete absence of any large floes. The mean size of the floes in the western area is more than an order of magnitude smaller than those in the eastern area, having typical dimensions of 1-2 km across, and they have an angular, fragmented shape. It is important to bear in mind that these images (Figure 5a and 5c) show ice at the same latitude and are essentially synoptic.

ERTS-1 images obtained on 1 August, 5 September and 8 September (Figure 5b) in approximately the same area as shown in Figure 5a also show no large floes but numerous small floes that appear to have undergone recent strong deformation. The general picture of this area given by the August and September ERTS-1 images is one of relatively small, angular ice floes undergoing strong dynamic activity with large strains occurring frequently.

We cannot tell the age of the numerous small floes observed in the western Beaufort Sea solely with the use of the ERTS-1 data since it is possible that many of the floes are fragmented multiyear floes. However, when we compare these images to the 1972 microwave images (Figures 3, 4, and 5) of the same area, we are tempted to conclude that the area in the summer and fall was largely made up of first-year ice, as it was during the spring.

ICE DRIFT BY MEANS OF ERTS-1 IMAGERY AND NIMBUS 4-IRLS PLATFORMS

An ERTS-1 image of the same area of the western Beaufort Sea as shown in Figure 5a was acquired one day earlier on 21 August 1972. Comparison of these

two images, in which numerous floes can be tracked, shows that considerable ice deformation occurred at this time. On 21 August there was a preferred N-S orientation of major leads, whereas on 22 August there was no preferred orientation but rather a random array of small leads. In the interval of one day, the triangular-shaped polynya shown in the southwest corner of Figure 5a, approximately 45 km north of the amorphous edge of the pack, had been stretched in an E-W direction and compressed in the N-S direction. The high resolution of the ERTS-1 imagery permits strains to be estimated, which in this case were very large with approximately 10% E-W stretching and approximately 6% N-S compression.

Figure 5b is a strip of ERTS-1 images obtained on 8 September of approximately the same area observed on 22 August (Figure 5a). The melt season was over at this time and newly frozen ice fills most of the leads. The floes in the western part of this mosaic resemble the numerous small floes visible in Figure 5a, but in the south-center section a N-S band of larger, rounded floes is seen. The origin of these large floes cannot be determined from the ERTS-1 pictures because sequential images of a given area can, at best, be obtained only on 3 successive days at 18-day intervals. It is, therefore, highly desirable to have additional data on the ice dynamics which should be obtained between the periods of ERTS-1 observations. As mentioned earlier, seven IRLS buoys were positioned around the manned drift station array of the 1972 experiment and left in place when the manned stations were vacated. These buoys continued to operate, giving daily coordinates and surface atmospheric pressure, throughout the following summer; five of them are still operating as of June 1973. The general drift trajectories of these buoys is shown in Figure 6. The data from

these buoys are stored in the AIDJEX data bank, and a report on the Beaufort Sea ice dynamics as deduced from IRLS data is under preparation by AIDJEX scientists (P. Martin, personal communication).

The IRLS ice drift data complement the ERTS-1 data in that they allow us to infer the ice dynamics that took place between successive satellite images. As a first example, let us return to Figures 5a and b. At the time these images were made, Buoy Number 6 (the buoy left at the vacated Main Camp) was located at the northern edge of each image. Its respective positions on 22 August and 8 September were 76°58'N - 151°56'W and 77°47'N - 154°29'W. Thus it moved 96 km to the NW during that period. Another Buoy, Number 2, which was drifting approximately 200 km to the west of the area of each image, experienced about the same drift toward the NW. Since we may assume that the differential motions within the area are less than the translation of the area itself, it appears that the larger floes shown in the center of Figure 5b were advected into the area from the east, and that at the time of the earlier image (Figure 5a) they were just east of the image area.

Another good example of the advantage of complementary ERTS-1 sequential images with Buoy tracking can be found in the case of the two large floes tracked from 17 August to 24 September in the eastern Beaufort Sea (Figure 6). Both floes had similar trajectories, and considerable relative strains occurred. During the 19 August to 4 September drift, the floes converged with an average strain rate of 2.3% per day, and during the 4-21 September drift they diverged with an average strain rate of 1.5% per day. These floes were situated at the edge of the ice pack and had much open water around them, thus deformation could easily occur. While these are large strains, they are less than those

observed at approximately the same time in the western Beaufort Sea as discussed earlier. During the drift period of these two floes another buoy, Number 3, was located approximately 360 km to the NW. During the period 17 August to 4 September, the buoy drifted SSW for 44 km while the tracked floes moved WNW, thus the area between them converged in the NW-SE direction and moved west. On the other hand, during the 4 to 22 September period, the buoy moved SSW for 75 km and the tracked floes moved south about equally which implies that a large area of the eastern Beaufort Sea ice pack had a uniform translation. Thus, we have demonstrated how the presence and absence of ice deformations can be derived from data obtained simultaneously by two different satellite techniques in adjacent areas.

Correlations between the drift of buoys and floes seen by ERTS-1 in the same area under conditions of pronounced ice drift have been established for short periods (2-3 days).

The ERTS-1 imagery and the buoy data agree that during the month of August the entire southern Beaufort Sea ice pack drifted mainly west, with the eastern area drifting toward the SW and the western area drifting toward the NW. An ERTS-1 image of an area of the Beaufort Sea located between the areas shown in Figures 5a and b (western sector) and 5c (eastern sector) was obtained on 27 August. It clearly shows numerous floes of an intermediate size between the large ones observed in the east and the small ones observed in the west, with an average size in the order of 10 km across.

Of all ERTS-1 images analyzed for the summer 1972 over the consolidated pack ice this image shows the largest amount of open water, estimated at 5% of the total area.

Considering these data, we find the ice of the southern Beaufort Sea to be a nonhomogeneous mixture of floe sizes, very large and rounded in the east and smaller but rounded in the center. Even smaller but angular floes appear in the western sector. The general direction of ice drift in the southern Beaufort Sea is to the west during this period. The 1971-72 experiment tempt us to conclude that the large eastern floes are multiyear and the small western ones are predominantly first-year.

NIMBUS 5 MICROWAVE SYNOPTIC OBSERVATIONS OF ARCTIC SEA ICE CANOPY

The Electronically Scanning Microwave Radiometer (ESMR) mounted on the Nimbus 5 satellite is providing synoptic images of microwave emission at 1.55 cm wavelength over the entire globe, including the Arctic. Two of these images are shown in Figure 7.

The image for 16 December 1972 shows low brightness temperatures throughout most of the Arctic Ocean with the exception of a large warm zone north of the coast of Alaska, a smaller one extending from north of the McKenzie Delta into the Amundsen Gulf, large warmer zones in the Laptev Sea and East Siberian Seas, with the largest and warmest zone in the Kara Sea. Based on the results of the AIDJEX experiments, the areas of low brightness temperatures are believed to be covered by multiyear ice and areas of high brightness temperatures by first year ice or a mixture of the two that is predominantly first-year. This assumption breaks down only where there is a mixture of high emissivity new year ice with extremely low emissivity open water, where the ice covered areas are smaller than the 30 × 30 km resolution of the radiometer. In

this case, the mixed composition of the area will produce a brightness temperature much higher than that of open water but lower than that of first year ice, namely corresponding to multiyear ice. The Bering Sea and Greenland Sea are typical for such areas in Figure 7. However, such open water areas which are partially covered with new year ice can easily be identified in sequential images where the overall brightness temperature will increase rapidly as the area becomes more and more covered with first year ice.

Based on this information we have identified various ice types in the two microwave images (Figure 7), as shown in Figure 8.

In the image obtained on 16 December 1972 (Figure 7), a broad tongue of multiyear ice extends south from the central Arctic Ocean into the eastern Beaufort Sea as far south as 72°N, adjacent to Banks Island and north of the McKenzie Delta. First-year ice, or a mixture of predominantly first-year and multiyear (which we will hereafter call first-year), extends into the western Beaufort Sea in a broad triangular zone with its base running along the coast from the McKenzie Delta to the Bering Strait, and its apex at approximately 78°N and 160°W. This distribution of ice types now inferred on a synoptic scale for the entire Beaufort Sea bears out the inferences made from the transect microwave image obtained during the 1972 experiment (Figure 3). The transition from first-year to multiyear ice at 160°W occurs at 78°N in the satellite image and at 79°N in the aircraft transect at approximately the same longitude. Combined aircraft and satellite data suggest that this distribution of ice types is a quasi-steady-state feature of the Beaufort Sea, at least for the winters 1971/72 and 72/73.

This inference is further supported by another Nimbus 5 microwave image acquired on 10 February 1972 (Figure 7).

Noting the Beaufort Sea in this image and its analysis in Figure 8, the same broad tongue of multiyear ice extends into the eastern Beaufort Sea from the central Arctic, and slightly cooler brightness temperatures are found between Greenland and the Pole. The triangular zone of first-year ice in the western Beaufort Sea seen earlier is still there but it has broadened and shifted slightly westward. Thus, the nonhomogeneous distribution of ice types seems to persist throughout the winter 1972/73, with slight fluctuations of the first-year ice zone of the western Beaufort region.

Analyzing the microwave images (Figure 7), we see that as the winter progressed the first-year ice in the East Siberian and Laptev Seas occupies the same area whereas the first-year ice zone in the Kara Sea has either expanded further north between Severnaya Zemlya and Franz Josef Land or the ice in that area was not consolidated earlier. Of all the Arctic Basin first-year ice zones observed in these images, the one in the western Beaufort Sea is the only one not bordered by islands and not located over shelves in shallow seas where lower surface water salinities exist at the time of freeze up. Therefore, the first-year zones north of Asia may result predominantly because they form in enclosed, shallow structured seas having large influxes of fresh water and hence low surface salinities, whereas the one north of Alaska may be the product of ice dynamics related to the behavior of the central Arctic Ocean ice.

Another pronounced variation of microwave emittance is observed over the Greenland ice cap (Figure 7). Brightness temperature variations of 50°C occur across the ice cap with the highest emittance corresponding roughly to the highest elevations of the central cap. Although we do not as yet fully understand the

cause of these brightness temperature variations occurring on glacier ice, we are certain that they are not due to variations in the physical temperature of the ice but rather are emissivity variations probably induced by variations of the small scale ice stands. We believe that these may be analogous to the emissivity variations between first year and multiyear sea ice. In that case the lower emissivity of multiyear ice is believed to be partly caused by the recrystallization due to seasonal thawing and refreezing. In the case of the glacier ice such crystal metamorphosis could be caused not only by temperature variations but also by pressure gradients within the ice.

CONCLUSIONS

This study illustrates how a variety of surface based, aircraft, and satellite observations can be combined and jointly analyzed to yield new findings which would not have resulted if the data were treated separately. We have found that ERTS-1 imagery can be used to study ice floe morphology and dynamics at time scales of several days to months and lead and polynya dynamics at scales of one to several days. Nimbus 4-IRLS drifting buoys have permitted the mapping of gross ice drift of the Beaufort Sea. They have also provided the continuity necessary for the derivation of pack ice motion occurring between intermittent ERTS-1 observations of a given area. The combining of buoy and imaged ice floe trajectories yielded information on gross ice deformation. Microwave (1.55 cm wavelength) images obtained during 1971 and 1972 experiments combined with those from Nimbus 5, permitted the delineation of first year and multiyear ice types at several scales over the entire Arctic.

During the 1971-73 period, the Beaufort Sea ice canopy consisted of non-homogeneously distributed floe sizes and types, with the eastern sector composed of large, rounded multiyear floes and the western sector composed of small, angular predominantly first-year floes. It appears that the strong dynamical activity of the general westward ice flow through the Beaufort Sea results in pronounced fracturing of the large multiyear floes that are advected into the eastern Beaufort Sea from the north.

The nonhomogeneous distribution of ice types, floe sizes and deformational strains, derived from this ensemble of observations implies that the western Beaufort Sea must be a zone of net annual ice divergence, from which the first-year ice that survives the summer melt would flow into the transpolar drift stream and/or the Beaufort Sea Gyre. In either case this ice would be transported northward from this area.

In order to prevent the net influx of multiyear ice during the summer season from the eastern Beaufort Sea which would occur under the presently held concept of a steady-state Gyre, the position and/or structure of the Gyre must undergo seasonal variations.

IN MEMORIUM

The data collected by the crew of the NASA CV-990 "Galileo" airborne observatory during their many Arctic Ocean missions were of key importance to this and other investigations of Arctic Sea ice. Their dedication and skilled labors have opened new frontiers of knowledge. We mourn the loss of some of these fine men as a result of the tragic crash of that aircraft on 12 April 1973.

ACKNOWLEDGEMENT

One of us (W. Campbell) was supported in this endeavor by the NOAA/NESS Spacecraft Oceanography Center under Contract No. NA-916-73.

REFERENCES

Barnes, James C. and J. Bowley (1973), "Use of ERTS Data for Mapping Arctic Sea Ice," Proceedings of the Earth Resources Technology Satellite-1 Symposium Proceedings, March 1973, in press.

Barnes, J. C., D. T. Chang, and J. H. Willand (1972), "Image Enhancement Techniques for Improving Sea Ice Depiction in Satellite Infrared Data," Journal of Geophysical Research, 77, pp. 453-462.

Budyko, M. I. (1968), "On the Origin of Glacial Epochs," (in Russian), Meteorol. Gidrol. (11).

Budyko, M. I. (1969), "Climate Changes," (in Russian), Hydrometeorological Publishing House, Leningrad.

Campbell, W. J. (1965), "The Wind-Driven Circulation of Ice and Water in a Polar Ocean," Journal of Geophysical Research, 70, pp. 3279-3301.

Campbell, W. J. (1971), "Remote Sensing Needs of Arctic Geophysics," Proceedings of the Seventh International Symposium on Remote Sensing of Environment, Willow Run Laboratories, pp. 937-940.

Campbell, W. J. (1972), "NASA Remote Sensing of Sea Ice in AIDJEX," Means of Acquisition and Communication of Ocean Data, Volume II, Surface, Subsurface, and Upper-air Observations, Proceedings of the WMO Technical Conference, October 1972, pp. 56-66.

Campbell, W. J. (1973), "Analysis of Arctic Ice Features," Earth Resources Technology Satellite-1 Symposium Proceedings, September 29, 1972, Goddard Space Flight Center, pp. 129-130.

Fletcher, J. O. (1965), "The Heat Budget of the Arctic Basin and its Relation to the Climate," The Rand Corporation (R-444-PR), pp. 179.

Fletcher, J. O. (1966), "Forward," Proceedings of the Symposium on the Arctic Heat Budget and Atmospheric Circulation, The Rand Corporation (RM-5233-NSF).

Fletcher, J. O. (1968), "The Polar Oceans and World Climate," Proceedings of the Long-Range Polar Objectives Conference, U.S. Department of Transportation, Washington, D.C.

Gloersen, P., W. Nordberg, T. C. Chang, T. J. Schmugge, W. J. Webster, T. T. Wilheit, and W. J. Campbell (1972), "Remote Observations of Microwave Radiation from Arctic Sea Ice during the 1971 and 1972 AIDJEX Expeditions," Symposium on Sea-Air Interaction in Polar Regions, American Geophysical Union, San Francisco, 1972.

Gloersen, P., W. Nordberg, T. J. Schmugge, T. T. Wilheit, and W. J. Campbell (1973), "Microwave Signatures of First-Year and Multiyear Sea Ice," Journal of Geophysical Research, 78, pp. 3564-3572.

Hibler, W. D. III, W. F. Weeks, S. Ackley, A. Kovacs, and W. J. Campbell (1972), "Mesoscale Strain Measurements on the Beaufort Sea Pack Ice (AIDJEX 1971)," AIDJEX Bulletin #13, pp. 35-76, (to be published in the Journal of Glaciology).

Hibler, W. D. III, W. F. Weeks, A. Kovacs, and S. Ackley (1973), "Differential Sea Ice Drift I, Spatial and Temporal Variations and Mesoscale Strain in Sea Ice." (To be published in the Journal of Glaciology.)

Laikhtman, D. L. (1958), "The Drift of Ice Fields (O Dreife Ledyanykh Polei)," Trudy Leningradskogo Gidrometeorol. In-ta (Transactions of the Leningrad Hydrometeorological Institute), No. 7, Leningrad.

McClain, E. Paul (1973), "Detection of Ice Conditions in the Queen Elizabeth Islands," Earth Resources Technology Satellite-1 Symposium Proceedings, September 29, 1972, Goddard Space Flight Center, pp. 127-129.

McClain, E. Paul and M. D. Baliles (1971), "Sea Ice Surveillance from Earth Satellites," Mariners Weather Log, 15 (1), pp. 1-4.

Maykut, G. A., A. S. Thorndike and N. Untersteiner (1972), "AIDJEX Scientific Plan," AIDJEX Bulletin #15.

Meeks, D., R. O. Ramseier, G. Poe, W. J. Campbell, and A. Edgerton (1972), "Preliminary Interpretation of Surface Based Microwave Measurements of Arctic Sea Ice," Symposium on Sea-Air Interaction in Polar Regions, American Geophysical Union, San Francisco, 1972, in press.

Mintz, Y. (1965), "Very Long Term Global Integration of the Primitive Equation of Atmospheric Motion," WMO Tech. Notes (66).

Nelson, H. P., S. Needham, and T. D. Roberts (1970), "Sea Ice Reconnaissance by Satellite Imagery," Final Report to the National Aeronautics and Space Administration, 1970.

Ruzin, M. I. (1959), "On the Wind-Induced Ice Drift in an Inhomogenous Pressure Field (O Vetrovom Dreife L'dov V Neodnorodnom Pole Davleniya)," Tr. Arkt. i Antarkt. In-ta i Glavn. Geofiz. Observ. (Transactions of the Arctic and Antarctic Institute and the Main Geophysical Observatory), T. 226, Leningrad.

Wilheit, T. T., W. Nordberg, J. Blinn, W. J. Campbell, and A. Edgerton (1972), "Aircraft Measurements of Microwave Emission from Arctic Sea Ice," Remote Sensing of Environment, 2 (3), pp. 129-139.

FIGURE CAPTIONS

Figure 1: Positions of NASA-AIDJEX experiments, showing also the drift track of Fletcher's Ice Island (T-3).

Figure 2: Comparison of ice morphology of western and eastern areas of the Beaufort Sea Ice as observed with an imaging microwave radiometer operating at a wavelength of 1.55 cm. The locations of main AIDJEX camps are indicated by the white circles. The white triangle indicates the position of the ice strain array during 1971 experiment.

Figure 3: Transect of the Beaufort Sea Ice Gyre (location shown in Figure 1) as observed with the 1.55 cm microwave imager on April 18, 1972. Again the main AIDJEX camp is indicated by a white circle.

Figure 4: Changes in the lead structure shown in microwave images of sea ice. The orientation of the leads is indicated by the white arrows. The white circles again indicate the location of the main AIDJEX camp.

Figure 5: ERTS-1 composite images of Beaufort Sea Ice obtained in the approximate positions of the 1971 and 1972 AIDJEX experiments.

Figure 6: Drift tracks of IRLS buoys in the Beaufort Sea. Also shown are the drift tracks of two large ice floes of Banks Island derived from ERTS-1 imagery.

Figure 7: Nimbus 5 microwave (λ = 1.55 cm) images of the Arctic.

Figure 8: Analysis of images shown in Figure 7.

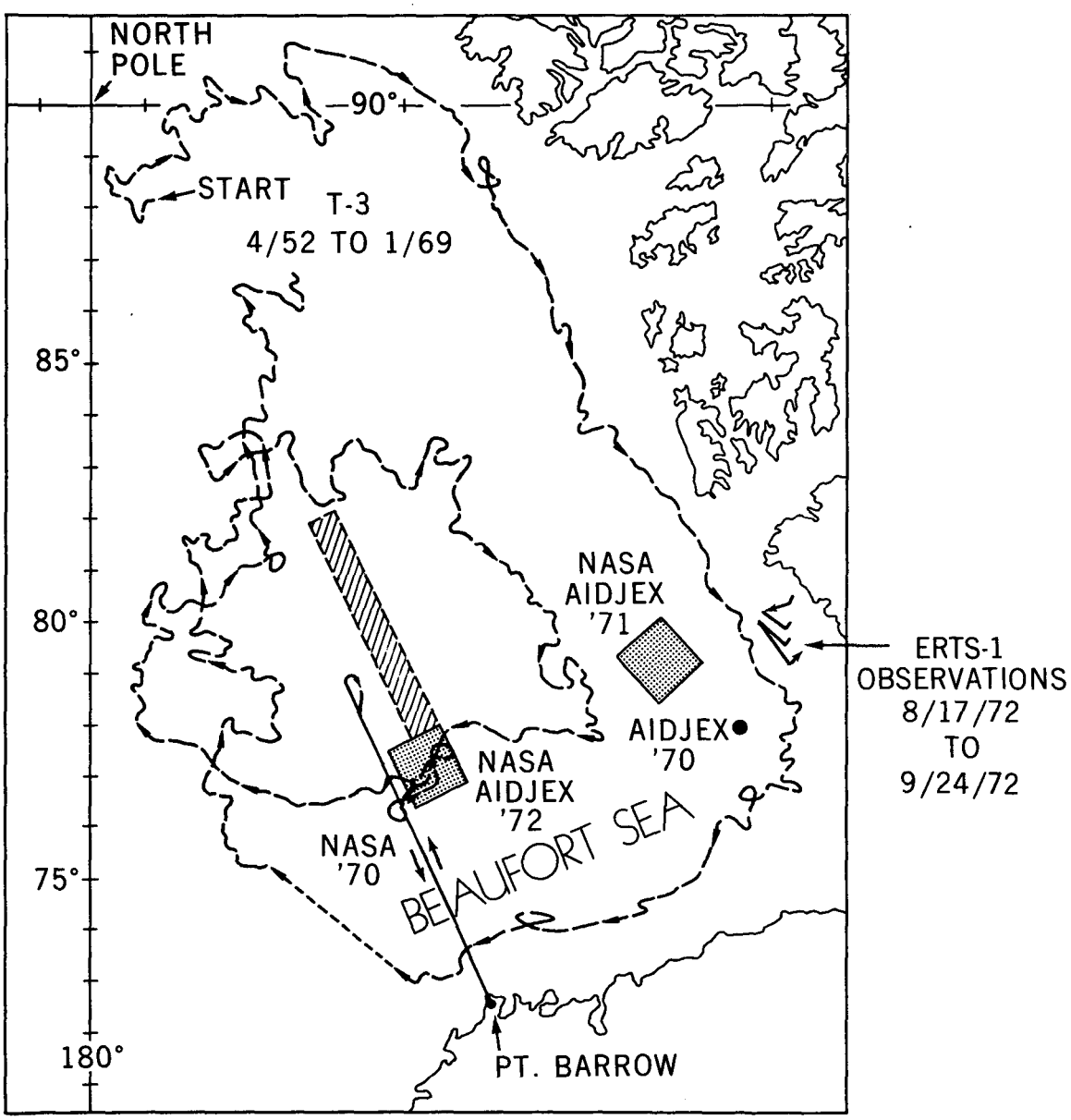
NORTH
POLE
90°
START
T-3
4/52 TO 1/69
85°
80°
75°
180°
NASA
AIDJEX
'71
AIDJEX
'70
NASA
AIDJEX
'72
NASA
'70
BEAUFORT SEA
PT. BARROW
ERTS-1
OBSERVATIONS
8/17/72
TO
9/24/72

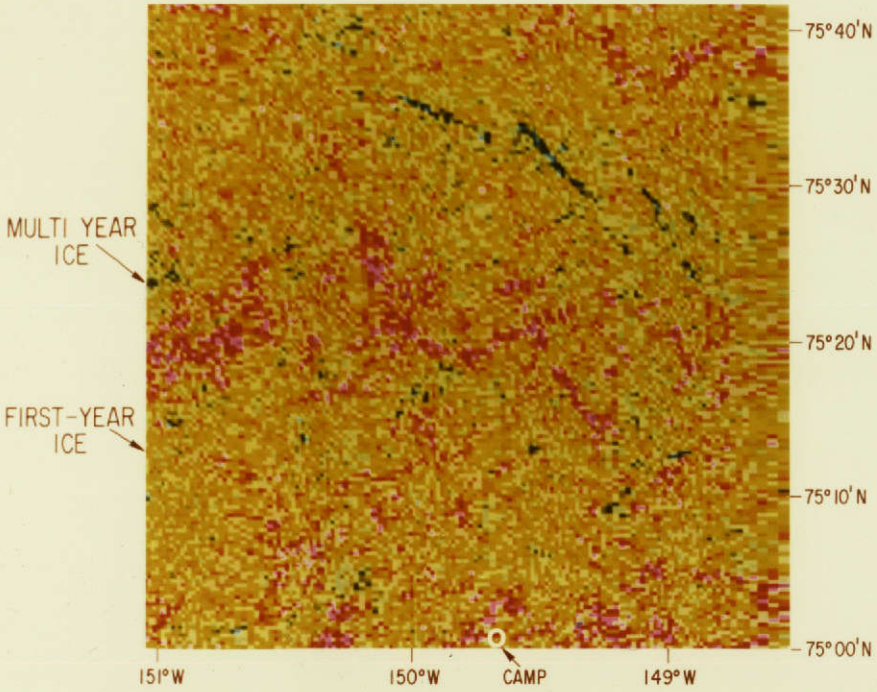

12 APRIL 1972
75° N 150° W

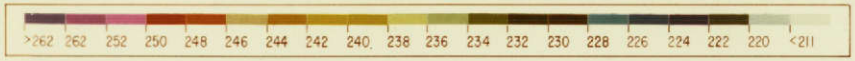

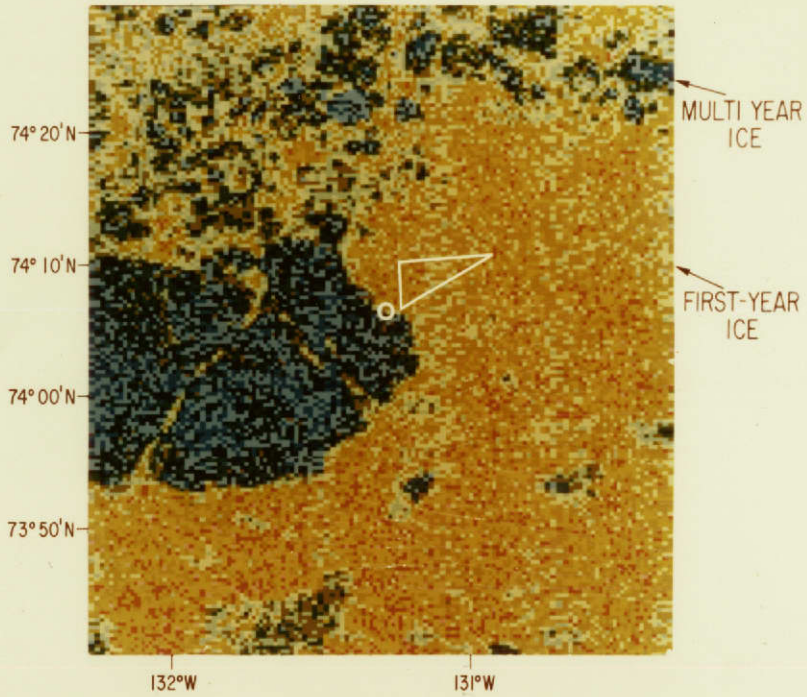

15 MARCH 1971
74° N 131° W

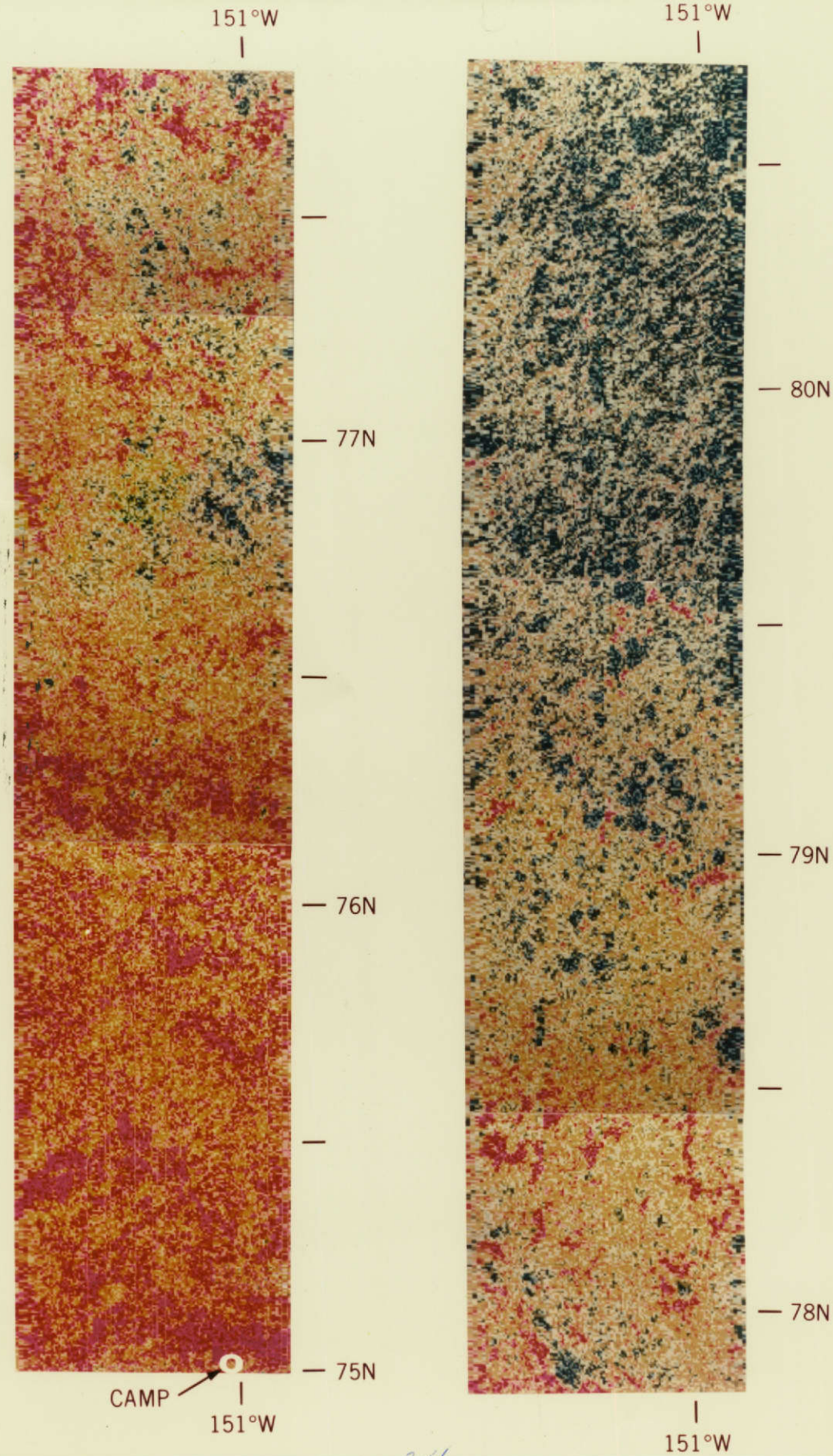
151°W
77N
76N
75N
CAMP
151°W
151°W
80N
79N
78N
151°W

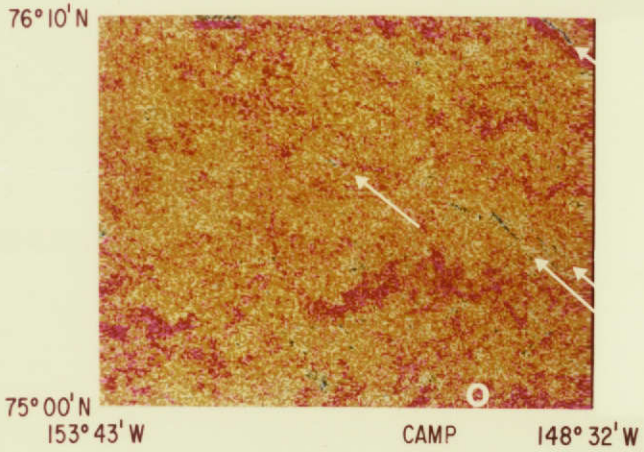

12 APRIL 1972

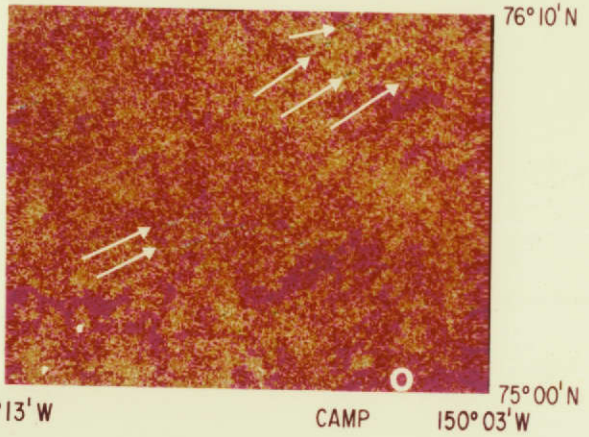

15 APRIL 1972

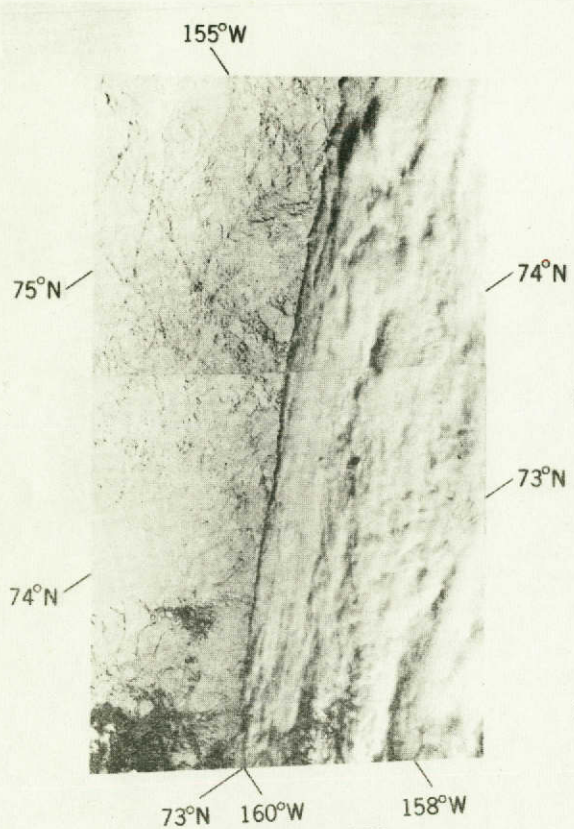

22 AUGUST 1972

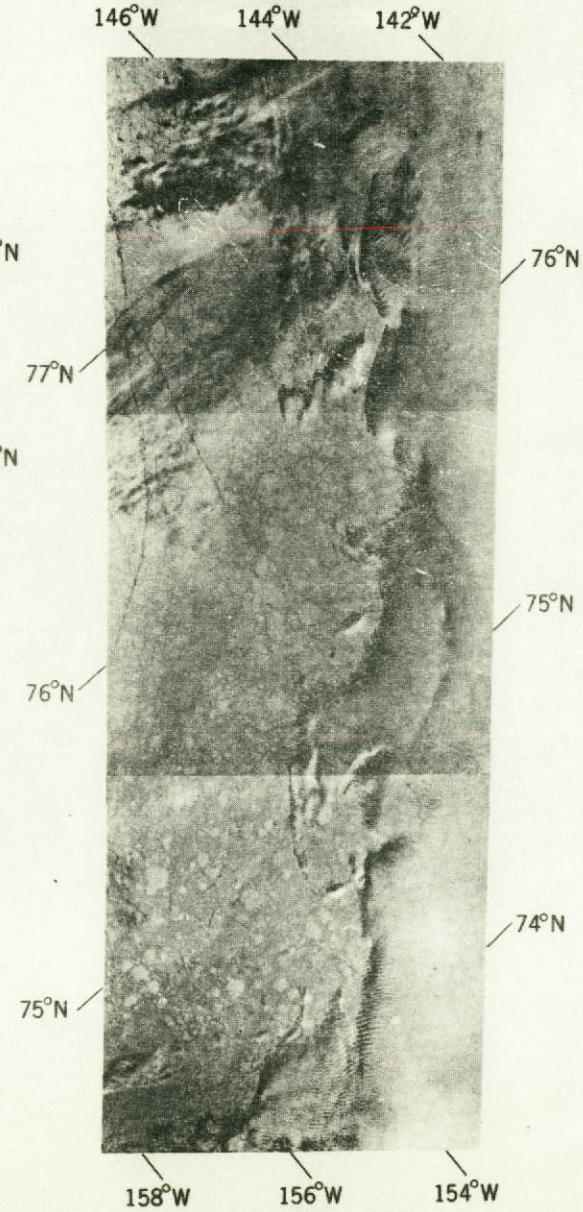

8 SEPTEMBER 1972

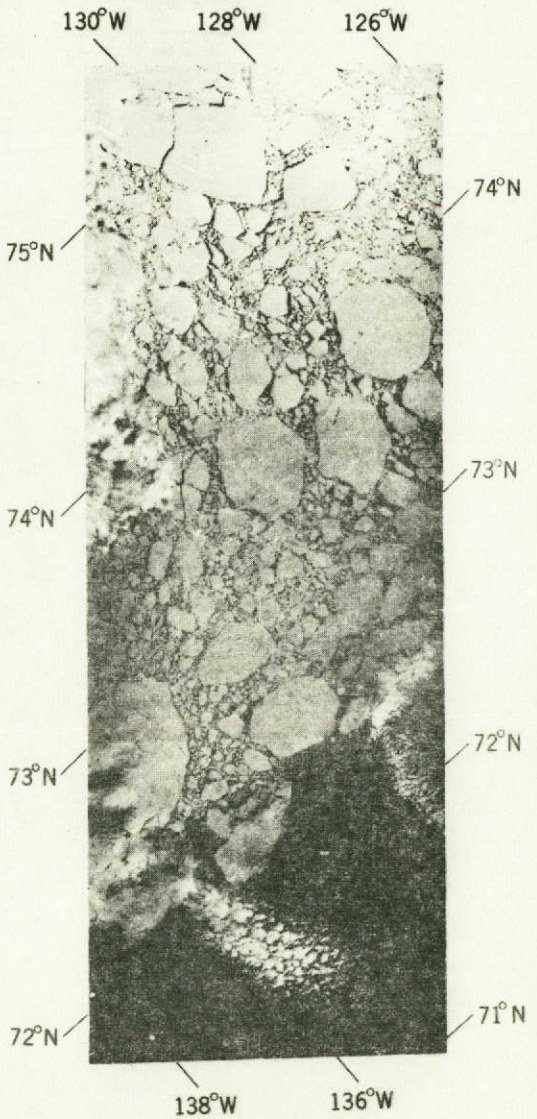

22 AUGUST 1973

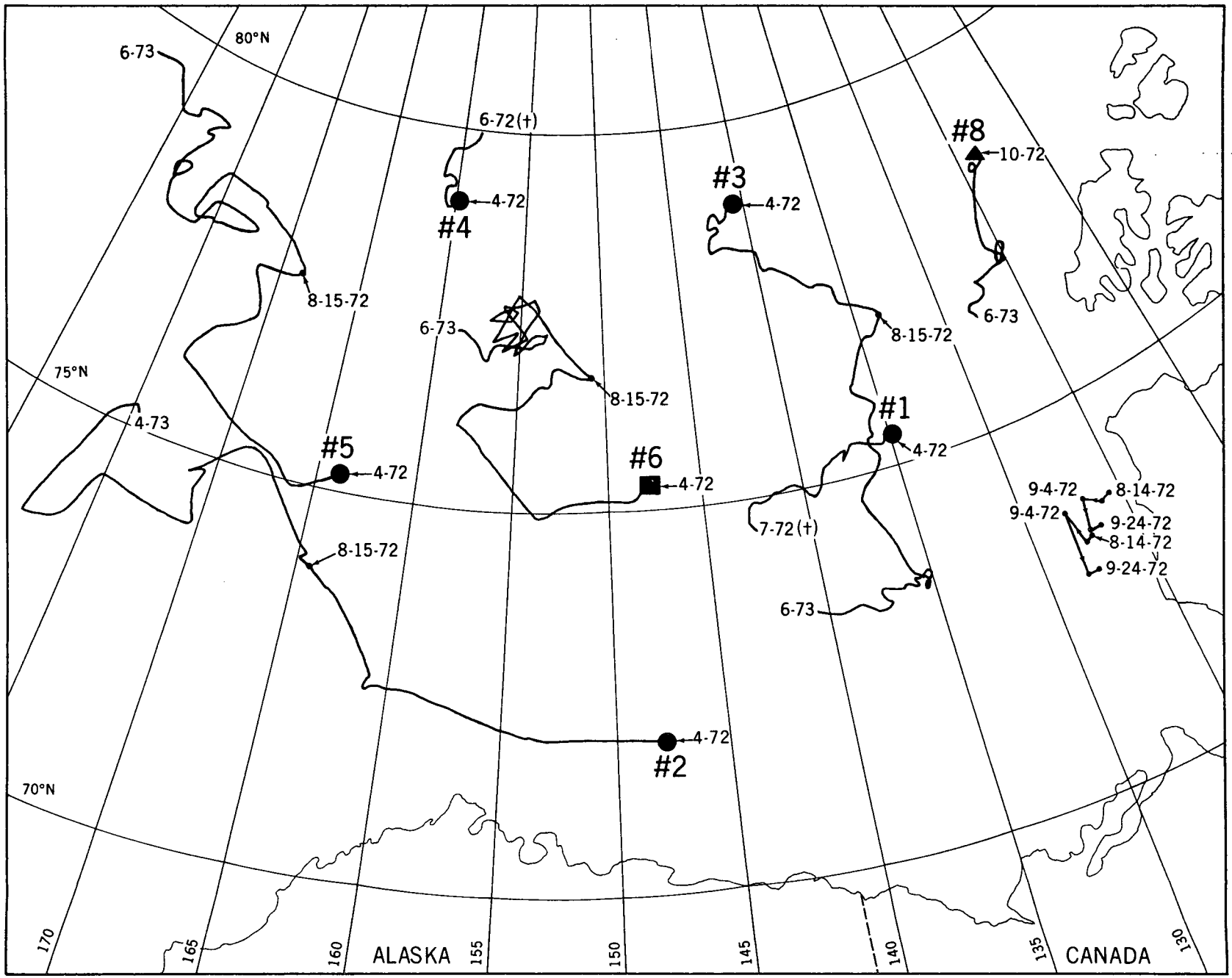
80°N
75°N
70°N
6-73
6-72(†)
#4
4-72
#3
4-72
#8
10-72
6-73
8-15-72
6-73
8-15-72
#1
4-72
4-73
#5
4-72
#6
4-72
9-4-72
8-14-72
9-4-72
9-24-72
8-14-72
9-24-72
7-72(†)
8-15-72
6-73
4-72
#2
170
165
160
ALASKA
155
150
145
140
135
CANADA
130

16 DECEMBER 1972

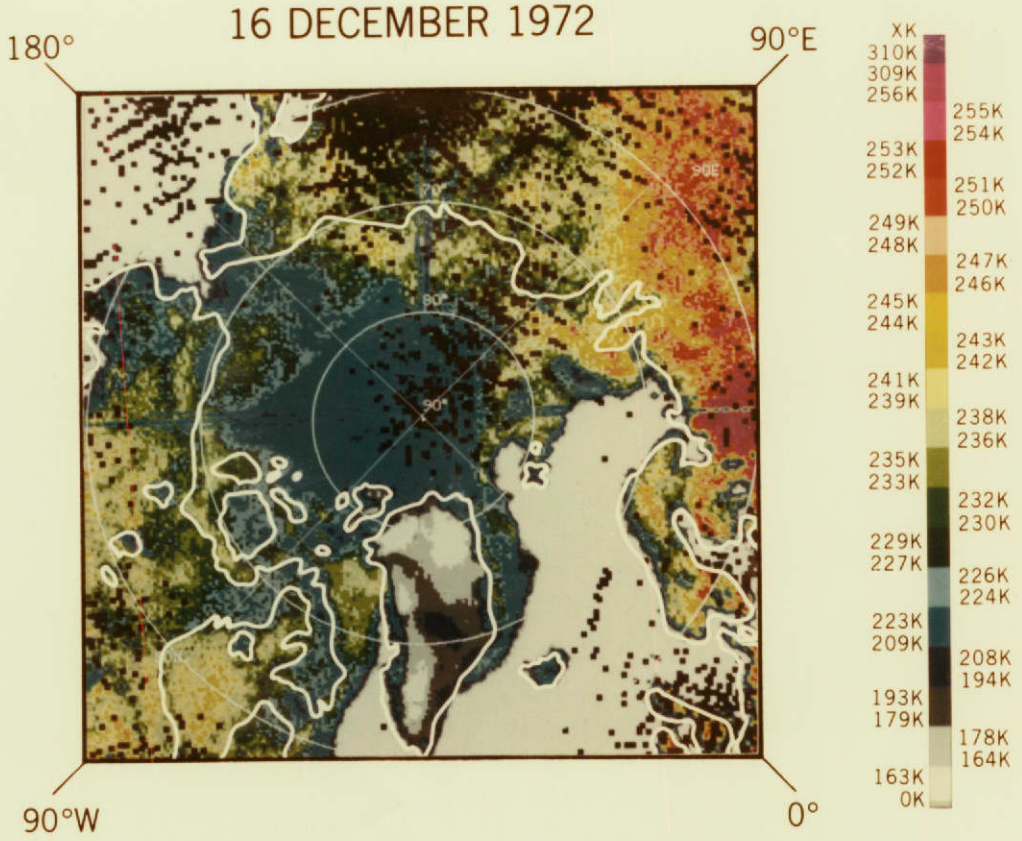

10 FEBRUARY 1973

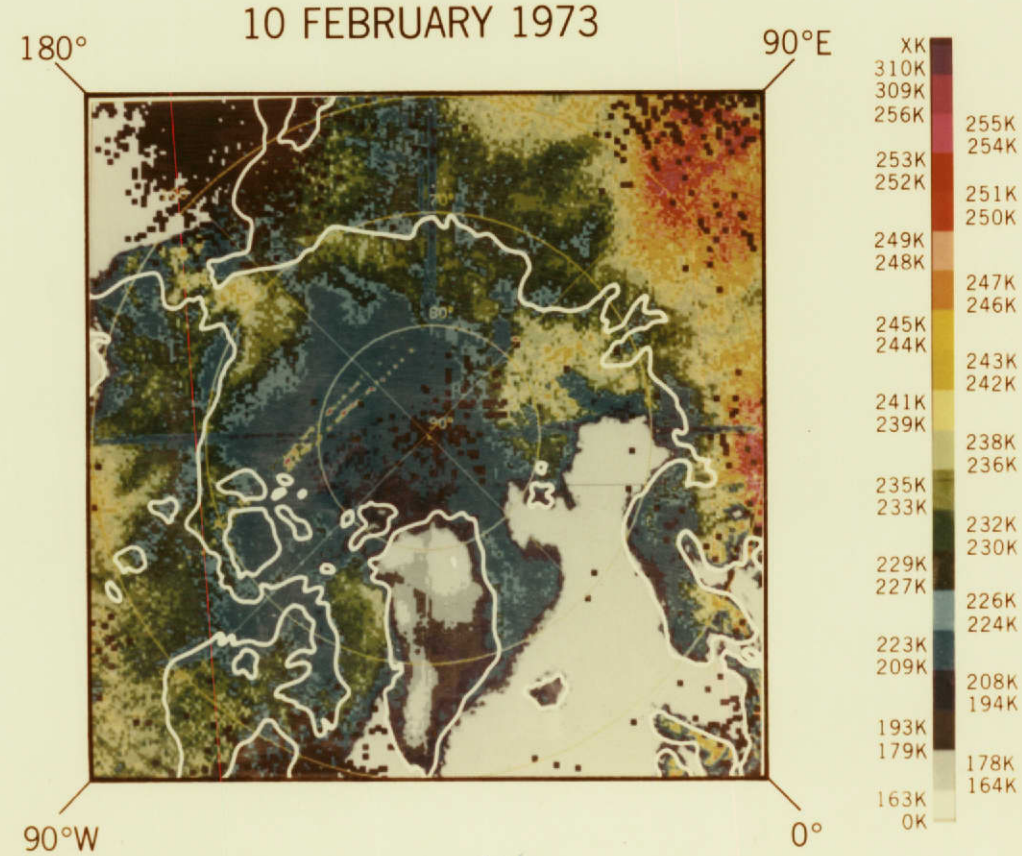

16 DECEMBER 1972

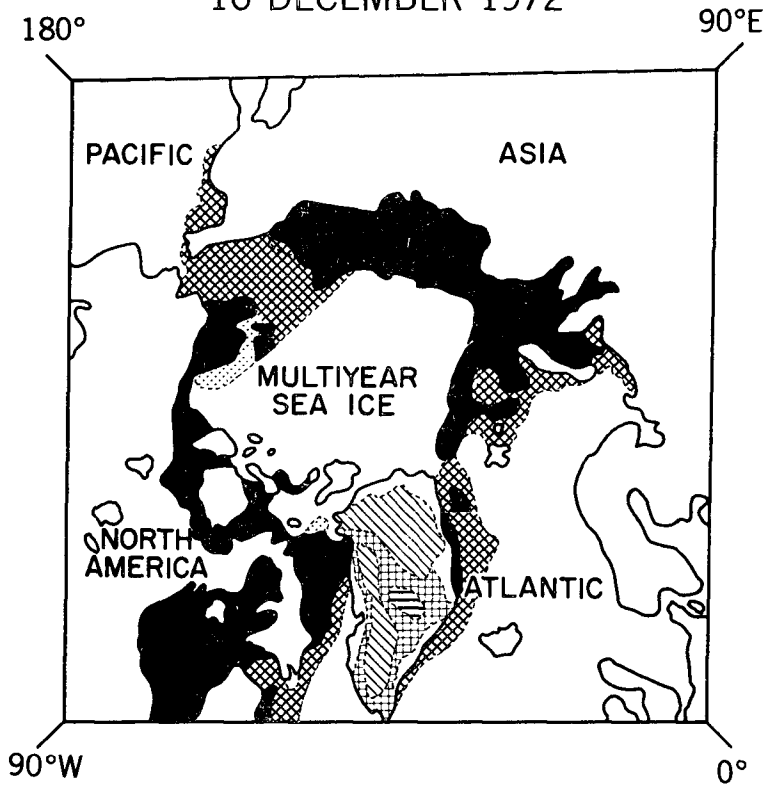

SEA ICE

FIRST YEAR

FIRST YEAR AND
MULTIYEAR MIXTURE

FIRST YEAR AND
OPEN WATER MIXTURE

10 FEBRUARY 1973

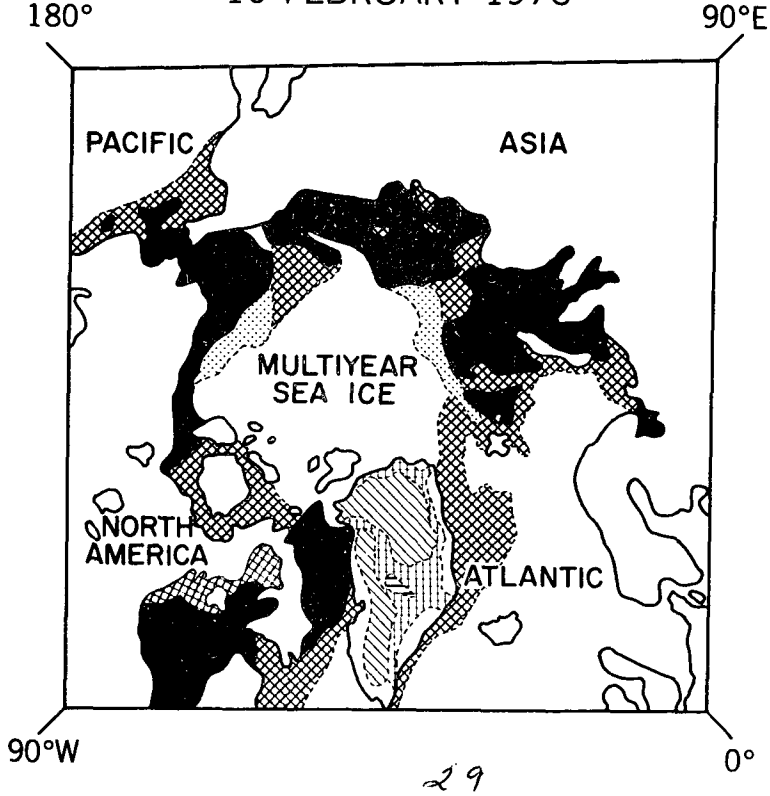

GLACIER ICE

≥ 178°K

179–193°K

194–208°K